



Contents lists available at ScienceDirect

Journal of Ginseng Research

journal homepage: <http://www.ginsengres.org>

Research Article

Two new triterpenoid saponins derived from the leaves of *Panax ginseng* and their antiinflammatory activityFu Li^{1,☆}, Yufeng Cao^{2,☆}, Yanyan Luo^{2,☆}, Tingwu Liu², Guilong Yan², Liang Chen², Lilian Ji², Lun Wang¹, Bin Chen¹, Aftab Yaseen¹, Ashfaq A. Khan³, Guolin Zhang¹, Yunyao Jiang⁵, Jianxun Liu⁵, Gongcheng Wang^{4,***}, Ming-Kui Wang^{1,**}, Weicheng Hu^{2,*}¹ Key Laboratory of Mountain Ecological Restoration and Bioresource Utilization and Ecological Restoration Biodiversity Conservation Key Laboratory of Sichuan Province, Chengdu Institute of Biology, Chinese Academy of Sciences, Chengdu, China² Jiangsu Collaborative Innovation Center of Regional Modern Agriculture & Environmental Protection/Jiangsu Key Laboratory for Eco-Agricultural Biotechnology Around Hongze Lake, Huaiyin Normal University, Huaian, China³ Department of Chemistry, Women University of Azad Jammu and Kashmir, Bagh, Pakistan⁴ Department of Urology, The Affiliated Huaian No. 1 People's Hospital of Nanjing Medical University, Huaian, China⁵ Xiyuan Hospital, China Academy of Chinese Medical Sciences, Beijing, China

ARTICLE INFO

Article history:

Received 26 July 2018

Received in Revised form

4 September 2018

Accepted 18 September 2018

Available online 4 October 2018

Keywords:

Antiinflammatory activity

Panax ginseng

Triterpenoid saponins

ABSTRACT

Background: The leaves and roots of *Panax ginseng* are rich in ginsenosides. However, the chemical compositions of the leaves and roots of *P. ginseng* differ, resulting in different medicinal functions. In recent years, the aerial parts of members of the *Panax* genus have received great attention from natural product chemists as producers of bioactive ginsenosides. The aim of this study was the isolation and structural elucidation of novel, minor ginsenosides in the leaves of *P. ginseng* and evaluation of their antiinflammatory activity *in vitro*. **Methods:** Various chromatographic techniques were applied to obtain pure individual compounds, and their structures were determined by nuclear magnetic resonance and high-resolution mass spectrometry, as well as chemical methods. The antiinflammatory effect of the new compounds was evaluated on lipopolysaccharide-stimulated RAW 264.7 cells.

Results and conclusions: Two novel, minor triterpenoid saponins, ginsenoside LS₁ (**1**) and 5,6-didehydroginsenoside Rg₃ (**2**), were isolated from the leaves of *P. ginseng*. The isolated compounds **1** and **2** were assayed for their inhibitory effect on nitric oxide production in LPS-stimulated RAW 264.7 cells, and Compound **2** showed a significant inhibitory effect with IC₅₀ of 37.38 μM compared with that of NG-monomethyl-L-arginine (IC₅₀ = 90.76 μM). Moreover, Compound **2** significantly decreased secretion of cytokines such as prostaglandin E₂ and tumor necrosis factor-α. In addition, Compound **2** significantly suppressed protein expression of inducible nitric oxide synthase and cyclooxygenase-2. These results suggested that Compound **2** could be used as a valuable candidate for medicinal use or functional food, and the mechanism is warranted for further exploration.

© 2018 The Korean Society of Ginseng, Published by Elsevier Korea LLC. This is an open access article under the CC BY-NC-ND license (<http://creativecommons.org/licenses/by-nc-nd/4.0/>).

1. Introduction

Ginseng (*Panax ginseng* Meyer) has been used as an herbal medicine or a functional food in East Asian countries because of its health-enhancing effects. The principle bioactive ingredients, termed ginsenosides, can be secreted from almost every part of this medicinal

plant [1]. However, the chemical compositions of the aerial and underground parts of *P. ginseng* differ significantly. The roots are rich in protopanaxdiol saponins (PPDs; e.g., the ginsenosides Rb₁, Rb₂, and Rc), whereas the leaves contain high levels of protopanaxtriol saponins (PPTs; e.g., the ginsenosides Rg₁ and Re) [2–4]. Pharmacological studies have demonstrated the different biological activities of these

* Corresponding author. Jiangsu Collaborative Innovation Center of Regional Modern Agriculture & Environmental protection/Jiangsu Key Laboratory for Eco-Agricultural Biotechnology Around Hongze Lake, Huaiyin Normal University, Huaian 223300, China.

** Corresponding author. Key Laboratory of Mountain Ecological Restoration and Bioresource Utilization and Ecological Restoration Biodiversity Conservation Key Laboratory of Sichuan Province, Chengdu Institute of Biology, Chinese Academy of Sciences, Chengdu 610041, China.

*** Corresponding author. Department of Urology, The Affiliated Huaian No. 1 People's Hospital of Nanjing Medical University, Huanghe West Road, Huaian, 223300, China

E-mail addresses: wgc1955@sina.com (G. Wang), wangmk@cib.ac.cn (M.-K. Wang), hu_weicheng@163.com (W. Hu).

☆ These authors equally contributed to this work.

two categories of ginsenosides. For example, the ginsenoside Rg₁ has been shown to induce angiogenesis, whereas Rb₁ exerted an opposite effect [5,6]. Thus, the roots and leaves of ginseng can be used for different medicinal purposes. Ginseng roots, the most commonly used part of the *P. ginseng* plant, have been extensively investigated. The leaves, which contain a higher level of total ginsenosides, have been relatively less studied [7].

In recent years, many ginsenosides with unique C-17 side chains have been isolated from the aerial components of ginseng [8–11]. In particular, the ginsenosides Rg₆, F₄, Rh₄, Rk₁, and Rg₅ were previously isolated from red ginseng in which the ginsenoside profile of ginseng products was altered by steaming [12–14]. These minor ginsenosides showed greater biological activities than the main constituents, such as ginsenosides Rg₁, Rc, and Rd [15,16]. In terms of cost and availability, ginseng leaves are more advantageous than the roots.

Inflammation is a clinically common and significant basic pathological process. Chronic inflammation may lead to many serious diseases. Nowadays, scientists are paying more and more attention to develop antiinflammatory agents from natural resources [17–19]. Some ginsenosides from the genus *Panax* also exhibited good antiinflammatory activities [20–22]. To adequately understand and explore the easily obtained ginseng leaves, this study focused on the isolation and antiinflammatory evaluation of previously undiscovered ginsenosides from this valuable source.

2. Materials and methods

2.1. Plant material and chemicals

Panax ginseng leaves were purchased in August 2013 from Jingyu County, Jilin Province, China. A voucher specimen (no. 20130820) of this plant was deposited in our laboratory. 1-(4,5-Dimethylthiazol-2-yl)-3,5-diphenylformazan and lipopolysaccharide (LPS) were obtained from Sigma-Aldrich (St. Louis, MO, USA). RPMI 1640 medium and antibiotics were obtained from Gibco BRL (Life Technologies, Shanghai, China). Fetal bovine serum was obtained from Corning (Mediatech, Inc., Manassas, VA, USA). NG-monomethyl-L-arginine was purchased from Beyotime (Haimen, China). Immun-Blot PVDF membrane for protein blotting (0.2 μm, #1620177) was acquired from Bio-Rad (Hercules, CA, USA). Primary antibodies including inducible nitric oxide synthase (iNOS; D6B6S, #13120), cyclooxygenase-2 (COX-2; D5H5, #12282), and β-actin (8H10D10, #3700) were acquired from Cell Signaling Technology (Beverly, MA, USA). Goat anti-rabbit IgG H&L (ab6721) and the enzyme-linked immunosorbent assay kits for prostaglandin E₂ (PGE₂) and tumor necrosis factor-α (TNF-α) were purchased from Abcam (Cambridge, MA, USA). The enhanced chemiluminescence Western blot kit, radio-immunoprecipitation assay (RIPA) lysis buffer, and bicinchoninic acid (BCA) protein assay kit were obtained from CWBIO (Taizhou, China). Silica gel (100–200 mesh) for open column chromatography (CC) was purchased from Qingdao Haiyang Chemical Group Co., Ltd. (Qingdao, China). Methanol (MeOH), acetonitrile (CH₃CN), *n*-butanol (*n*-BuOH), and dichloromethane (CH₂Cl₂) were purchased from Chengdu Kelong Chemical Co., Ltd. (Chengdu, China).

2.2. General experimental procedures

Optical rotations were measured using a PerkinElmer 341 polarimeter (PerkinElmer, MA, US). Infrared (IR) spectra were obtained using a PerkinElmer 1725X-FT spectrometer with potassium bromide disks. The high resolution electrospray ionization mass spectroscopy (HRESIMS) spectra were acquired on a Vion IMS QToF (Waters Corp., Milford, Massachusetts, USA) in positive ion mode. One-dimensional (1D) and two-dimensional (2D) NMR data were obtained using a Bruker Avance-600 spectrometer in C₅D₅N. Analysis of the sugar

residues by HPLC was carried out on an Alltech series III apparatus with an evaporative light-scattering detector with a COSMOSIL Sugar-D packed column (Nacalai Tesque, Inc., Tokyo, Japan) using a mobile phase of 80% acetonitrile (CH₃CN). Preparative-scale HPLC was implemented on a CXTH system, equipped with a C₁₈ column (50 × 250 mm i.d., 10 μm, Daiso SP-100-10-ODS-P) from Daiso Co., Ltd. (Osaka, Japan) at a flow rate of 90 mL/min.

2.3. Extraction and isolation

The leaves (100.0 kg) of *P. ginseng* plants were powdered and extracted with 80% MeOH (3 × 250 L, each 24 h) at 60°C. The concentration of the extract was implemented under a rotary evaporator (R-114, Buchi, Switzerland) to yield a dark residue, which was suspended in H₂O and partitioned successively with CH₂Cl₂ (3 × 15 L) and *n*-BuOH (3 × 15 L) to generate CH₂Cl₂ (1.1 kg) and *n*-BuOH (4.2 kg) soluble fractions.

A portion of the *n*-BuOH (4.0 kg) extract was applied to silica gel CC for separation using an H₂O-saturated CH₂Cl₂/MeOH solvent system (gradient: 15:1 to 1:1) to generate 12 fractions (Fr.1 to Fr.12). Fr.2 (32.6 g) was purified by preparative HPLC and eluted with 58% and 80% MeOH, producing five subfractions (Fr.2-1 to Fr.2-5). Fr.2-1 (5.6 g) was further purified by preparative HPLC using 35% CH₃CN to yield Compound **1** (*t*_R = 33.8 min, 26 mg). Fr.4 (40 g) was fractionated by preparative HPLC using 68%, 80%, and 90% MeOH as eluent to generate nine subfractions (Fr.4-1 to Fr.4-9). Further separation of Fr.4-6 (2.3 g) by preparative HPLC with 65% CH₃CN yielded Compound **2** (*t*_R = 27.4 min, 43 mg).

2.4. Spectroscopic data

Ginsenoside LS₁ (**1**): amorphous white powder; [α]_D²⁰ +20.7° (c 0.11, MeOH); IR_{vmax} 3393, 2950, 2351, 1386, 1305, 1078, 1036, 931, 894, and 655 cm⁻¹; ¹H-NMR (600 MHz, C₅D₅N) and ¹³C-NMR (150 MHz, C₅D₅N) data are shown in Table 1; *m/z* 659.4144 [M+Na]⁺ (calculated for C₃₆H₆₀O₉) from HRESIMS.

5,6-Didehydroginsenoside Rg₃ (**2**): amorphous white powder; [α]_D²⁰ +7.1° (c 0.15, MeOH); IR_{vmax} 3362, 2925, 2351, 1447, 1376, 1078, 1028, 896, and 655 cm⁻¹; ¹H-NMR (600 MHz, C₅D₅N) and ¹³C-NMR (150 MHz, C₅D₅N) data are shown in Table 1; *m/z* 805.4741 [M+Na]⁺ (calculated for C₄₂H₇₀O₁₃) from HRESIMS.

2.5. Determination of the absolute configurations of sugar moieties

The previously described method was used to determine the absolute configurations of the sugar residues [23]. Compounds **1** and **2** (5 mg each) were mixed and heated with 5% sulfuric acid (2 mL) at 105°C for 8 h. The resultant reaction mixture was exhaustively leached with CH₂Cl₂. Then, the water part was neutralized with barium hydroxide, filtered, and subjected to HPLC analysis compared to a standard glucose sample. The determined optical rotation value of [α]_D²⁰ +48.8° (c 0.05, H₂O) suggested the D-form for the glucose moieties in the identified compounds.

2.6. Cell lines and cell culture

RAW 264.7 cells were maintained in RPMI 1640 medium containing 10% fetal bovine serum and 1% antibiotics at 37°C under 5% CO₂/95% air.

2.7. Cell viability assay

RAW 264.7 macrophage cells (1 × 10⁵ cells/well) were seeded into 96-well plates and cultured for 18 h. Then, the culture medium was replaced with fresh medium along with the test compounds at

Table 1
¹H and ¹³C NMR (600 MHz, 150 MHz in C₅D₅N) data for Compounds **1** and **2**

Position	1		2	
	δ_{H}	δ_{C}	δ_{H}	δ_{C}
1	1.05, 1.73 (m)	39.4 (CH ₂)	0.93, 1.68 (m)	39.8 (CH ₂)
2	1.86, 1.96 (overlap)	28.2 (CH ₂)	1.92, 2.26 (overlap)	27.0 (CH ₂)
3	3.53 (dd, <i>J</i> = 11.4, 4.6 Hz)	78.6 (CH)	3.35 (dd, <i>J</i> = 11.5, 4.4 Hz)	88.0 (CH)
4		40.4 (C)		43.1 (C)
5	1.23 (d, <i>J</i> = 10.4 Hz)	61.8 (CH)		147.2 (C)
6	4.42 (m)	67.8 (CH)	5.63 (brs)	119.9 (CH)
7	1.88, 1.98 (overlap)	47.4 (CH ₂)	1.73, 2.07 (overlap)	34.9 (CH ₂)
8		41.3 (C)		37.2 (C)
9	1.58 (overlap)	49.9 (CH)	1.73 (overlap)	47.5 (CH)
10		39.4 (C)		37.4 (C)
11	1.57, 2.13 (overlap)	31.0 (CH ₂)	1.10, 1.62 (overlap)	32.1 (CH ₂)
12	3.97 (m)	70.7 (CH)	3.93 (overlap)	70.7 (CH)
13	2.04 (overlap)	49.2 (CH)	2.06 (overlap)	48.7 (CH)
14		51.6 (C)		51.3 (C)
15	0.98, 1.57 (overlap)	30.7 (CH ₂)	1.74, 2.07 (overlap)	33.8 (CH ₂)
16	1.42, 1.78 (overlap)	26.6 (CH ₂)	1.45, 2.02 (overlap)	27.0 (CH ₂)
17	2.39 (m)	52.3 (CH)	2.40 (m)	54.8 (CH)
18	1.05 (s)	17.5 (CH ₃)	0.95 (s)	17.8 (CH ₃)
19	1.15 (s)	17.5 (CH ₃)	1.12 (s)	20.4 (CH ₃)
20		83.3 (C)		73.1 (C)
21	1.59 (s)	23.6 (CH ₃)	1.46 (s)	27.3 (CH ₃)
22	2.85 (dd, <i>J</i> = 14.2, 8.6 Hz)	40.2 (CH ₂)	1.73, 2.02 (overlap)	36.2 (CH ₂)
23	3.10 (dd, <i>J</i> = 14.2, 6.5 Hz)			
24	6.08 (m)	127.5 (CH)	2.31, 2.61 (m)	23.1 (CH ₂)
25	6.42 (d, <i>J</i> = 15.6 Hz)	136.0 (CH)	5.33 (m)	126.4 (CH)
26		142.6 (C)		130.9 (C)
27	5.04 (s)	115.0(CH ₂) (CH ₂)	1.67 (s)	25.9 (CH ₃)
28	4.98 (s)			
29	1.93 (s)	19.0 (CH ₃)	1.65 (s)	17.7 (CH ₃)
30	1.99 (s)	32.1 (CH ₃)	1.52 (s)	28.2 (CH ₃)
31	1.47 (s)	16.6 (CH ₃)	1.45 (s)	24.2 (CH ₃)
32	0.91 (s)	17.2 (CH ₃)	1.04 (s)	16.8 (CH ₃)
3 or 20-Glc				
1	5.20 (d, <i>J</i> = 7.7 Hz)	98.4 (CH)	4.89 (d, <i>J</i> = 7.4 Hz)	105.0 (CH)
2	4.00 (t, <i>J</i> = 8.6 Hz)	75.4 (CH)	4.22 (overlap)	83.6 (CH)
3	4.23 (t, <i>J</i> = 9.0 Hz)	78.8 (CH)	4.24 (overlap)	78.1 (CH)
4	4.16 (t, <i>J</i> = 9.0 Hz)	71.6 (CH)	4.15 (overlap)	71.8 (CH)
5	3.93 (m)	78.5 (CH)	4.31 (overlap)	78.4 (CH)
6	4.34 (dd, <i>J</i> = 11.8, 5.4 Hz)	62.9 (CH ₂)	4.35, 4.48 (overlap)	62.9 (CH ₂)
	4.51 (dd, <i>J</i> = 11.8, 1.8 Hz)			
1'			5.36 (d, <i>J</i> = 7.6 Hz)	106.2 (CH)
2'			4.15 (overlap)	77.1 (CH)
3'			4.24 (overlap)	78.0 (CH)
4'			4.32 (overlap)	71.7 (CH)
5'			3.90 (overlap)	78.3 (CH)
6'			4.35, 4.53 (overlap)	62.8 (CH ₂)

various concentrations for 24 h. Cytotoxicity was investigated by 1-(4,5-dimethylthiazol-2-yl)-3,5-diphenylformazan assay as previously described [24]. Cell viability was expressed as a percentage of control cells.

2.8. Determination of NO, PGE₂, and TNF- α production

RAW 264.7 macrophage cells (1×10^5 cells/well) were cultured for 18 h in a 96-well plate; the cells were pretreated with different concentrations of test samples for 30 min before treatment with LPS for 24 h. Nitrite contents were determined by the Griess reaction. The contents of TNF- α and PGE₂ were evaluated according to the instruction on the kits.

2.9. Western blot analysis

RAW 264.7 cells were seeded onto 60-mm plates at 5×10^6 cells/well. After treatment, the cells were washed with cold phosphate buffered saline (PBS), and the whole protein was extracted with RIPA lysis buffer containing protease inhibitor cocktail tablets (Complete ultra, Roche, Germany) under a FastPrep-24 homogenizer (MP,

Solon, OH) with glass beads. Equal amounts of proteins were separated using 10% sodium dodecyl sulfate polyacrylamide gel electrophoresis and transferred onto a polyvinylidene fluoride (PVDF) membrane. The transferred protein was detected by iNOS (1:1000 dilution), COX-2 (1:1000 dilution), and β -actin (1:1000 dilution) using an enhanced chemiluminescence Western blot kit. The bands were visualized and photographed using the Tanon-5200 multi-imaging system (Tanon Science & Technology, Shanghai, China).

2.10. Data analysis

The values are presented as the mean \pm standard derivation. Differences between various experimental and control groups were compared using one-way analysis of variance followed by unpaired Student *t* test, and *p*-values less than 0.05 were considered significant.

3. Results and discussion

Separation of the *n*-BuOH fraction of *P. ginseng* leaves by open silica gel CC and preparative reversed HPLC yielded Compounds **1** and **2** (Fig. 1). Compound **1**, an amorphous white power, had a

molecular formula of $C_{36}H_{60}O_9$, which was based on the m/z of 659.4144 $[M+Na]^+$ determined in the HRESIMS analysis. Thin layer chromatography visualization by heating at $105^\circ C$ after spraying with 5% H_2SO_4 ethanol solution and the ^{13}C -NMR spectrum of Compound **1** suggested that it was a triterpene glycoside. The 1H -NMR spectrum of **1** revealed one anomeric proton signal at δ_H 5.20 (d, 7.7 Hz), whereas the ^{13}C -NMR spectrum displayed one anomeric carbon signal at δ_C 98.4. The sugar residue was determined as D-glucose by acid hydrolysis experiment. The β configuration for the glucose residue was verified according to the coupling constant of the anomeric proton. The signals at δ_H 4.98 (s), 5.04 (s), 6.08 (m), and 6.42 (d, 15.6 Hz) in the 1H -NMR spectrum, along with the signals at δ_C 127.5 (C-23), 136.0 (C-24), 142.6 (C-25), and 115.0 (C-26) in the ^{13}C -NMR spectrum suggested the presence of two double bonds in **1**. Compound **1** showed a maximum absorbance at 230 nm in its UV spectrum, indicating that the two double bonds were conjugated. Comparison of the ^{13}C -NMR data of **1** with those of quinquenoside L_1 demonstrated that they shared similar aglycones [25]. The appearance of carbon signals at δ_C 61.8 (C-5) and 67.8 (C-6) in **1** rather than at around δ_C 56.1 (C-5) and 18.2 (C-6) suggested the existence of a hydroxyl group at C-6 in **1** [8]. The 1H - and ^{13}C -NMR signals of compound **1** were further assigned by extensive two-dimensional NMR spectra. The heteronuclear multiple bond correlation (HMBC) correlation between H-1 (δ_H 5.20) of the glucose residue and C-20 (δ_C 83.3) of the aglycone suggested the location of the sugar residue (Fig. 2). The positions of the two double bonds in the side chain were confirmed by correlations between H₁-23 (δ 6.08) and C-22 and C-25 (δ 40.2 and 142.6); H₁-24 (δ 6.42) and C-22, C-25, and C-27 (δ 40.2, 142.6, and 19.0); H₂-26 (δ 4.98 and 5.04) and C-24 and C-27 (δ 136.0 and 19.0); and H₃-27 (δ

1.93) and C-24, C-25, and C-26 (δ 136.0, 142.6, and 115.0). Accordingly, Compound **1** was identified and named ginsenoside LS_1 .

Compound **2**, an amorphous white powder, possessed a molecular formula of $C_{42}H_{70}O_{13}$, which was based on the m/z of 805.4741 $[M+Na]^+$ determined in the HRESIMS analysis. Thin layer chromatography and ^{13}C -NMR analysis demonstrated that Compound **2** was also a triterpene glycoside. The 1H - and ^{13}C -NMR spectra of **2** exhibited signals that could be assigned to two sugar moieties at δ_H 4.89 (d, 7.4 Hz), 5.36 (d, 7.6 Hz) and δ_C 105.0, 106.2, respectively. Acid hydrolysis of **2** indicated that D-glucose was the only sugar component. The β configuration for both of the glucose residues was determined as described previously. The 1H -NMR spectrum of **2** showed signals due to eight tertiary methyl residues at δ_H 0.95, 1.04, 1.12, 1.45, 1.46, 1.52, 1.65, and 1.67 and two olefinic protons at δ_H 5.33 and 5.63 for the aglycone moiety. The existence of two double bonds in **2** was suggested from corresponding signals at δ_C 119.9, 126.4, 130.9, and 147.2 in the ^{13}C -NMR spectrum. Comparison of the NMR data of **2** with those of 5,6-didehydroginsenoside Rd indicated they had comparable chemical structures except for the absence of the glucose residue at C-20 in **2** [26]. Sugar sequence was indicated to be a 1 \rightarrow 2 linkage type attaching to C-3 of the aglycone from the HMBC correlations between δ_C 88.0 (C-3) and δ_H 4.89 (H-1 of the glc) and δ_C 83.6 (C-2 of the glc) and δ_H 5.36 (H-1 of the glc') (Fig. 2). The chemical shifts of C-17, C-21, and C-22 observed at δ_C 54.8, 27.3, and 36.2, respectively, suggested that the configuration of C-20 was S [27]. As a result, Compound **2** was identified and named 5,6-didehydroginsenoside Rg_3 .

Macrophages play a key role in the process of inflammation on account of their functions in innate immunity and adaptive

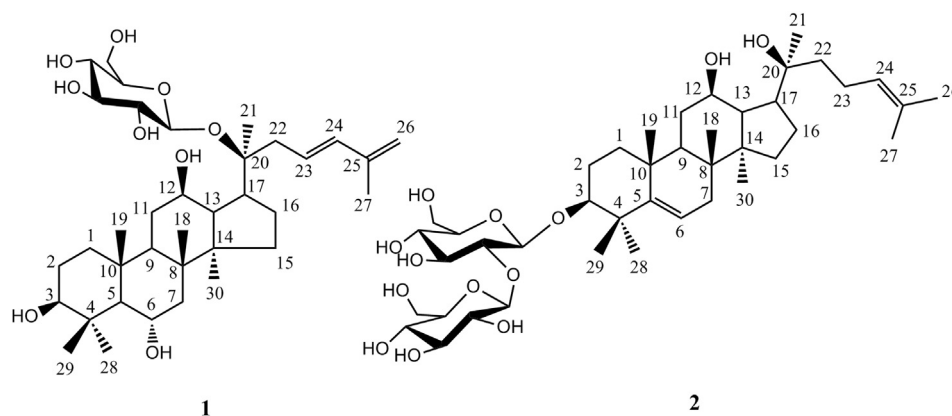


Fig. 1. Chemical structures of Compounds **1** and **2** isolated from the leaves of *Panax ginseng*.

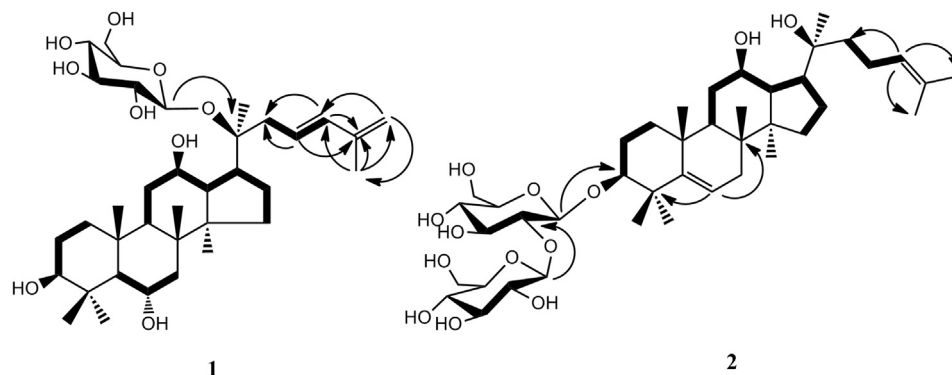


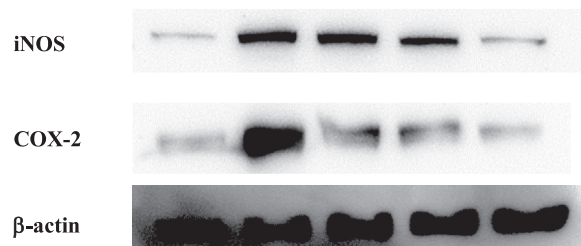
Fig. 2. Key HMBC (arrow) and 1H - 1H COSY (bold) correlations of Compounds **1** and **2**. COSY, correlation spectroscopy.

immunity. The activated macrophages by bacterial LPS initiate defensive reactions and release inflammatory mediators including NO and PGE₂ and proinflammatory cytokines such as TNF- α , interleukin 1 β (IL-1 β), and interleukin 6 (IL-6) to improve the defensive ability [28]. Overproduction of NO can be harmful and mediate a broad spectrum of inflammatory disorders. Therefore, the LPS triggered the release of NO in RAW 264.7 cells is an excellent model to assess the effects of drugs on the inflammatory process [29].

As shown in Fig. 3A, the nitrite concentration in unstimulated RAW 264.7 cells was almost undetectable; however, the nitrite concentration was increased significantly upon the treatment of LPS. Among the two compounds, Compound 2 significantly reduced NO production in LPS-stimulated RAW 264.7 with IC₅₀ value of 37.38 μ M, which was more potent than the positive control (L-NMA, 90.76 μ M), whereas Compound 1 did not exert an inhibitory effect.

To exclude the possibility that the cytotoxicity of Compound 2 might contribute to its antiinflammatory effects, we incubated RAW 264.7 cells with varying concentrations of Compound 2 for 24 h. As shown in Fig. 3B, Compound 2 treatment did not induce cell death in RAW 264.7 cells at concentrations up to 100 μ M. Furthermore, the levels of PGE₂ and TNF- α were determined using an enzyme-linked immunosorbent assay kit. As shown in Fig. 3C and D, Compound 2 inhibited TNF- α and PGE₂ production in a concentration-dependent manner.

Several ginsenosides, such as ginsenosides Rg1, Rf, Rh1, Rh2, Rb1, Rb2, Rc, Rd, Rg3, and Rg5, were previously reported to exert good antiinflammatory activities [30–35]. Ginsenosides Rg1, Rf, and Rh1 (PPT) shared one or two glucose residues at C-6. Ginsenosides Rh2, Rb1, Rb2, Rc, Rd, Rg3, and Rg5 (PPD) had one or two



LPS (1 μ g/mL)	-	+	+	+	+
Concentration (μ M)	-	-	25	50	100

Fig. 4. Effects of Compound 2 on the expression of iNOS and COX-2. (A) Cells were plated at a density of 5×10^6 cells/dish. Cells were pretreated with various concentrations of Compound 2 for 30 min before treatment with LPS for 6 h. After preparation of the whole protein, the protein expression levels of iNOS and COX-2 were measured by Western blot. Results are representative of three experiments. COX-2, cyclooxygenase-2; iNOS, inducible nitric oxide synthase; LPS, lipopolysaccharide.

glucose moieties at C-3 position. This conclusion also well fit the results of the present article. Compound 1 (PPT) had no glucose residues at C-6 and did not exhibit antiinflammatory activity, whereas Compound 2 (PPD) bore two glucose moieties at C-3 and showed excellent antiinflammatory activity.

iNOS is a product of transcription expression of activated macrophages and is the reason for the prolonged and profound production of NO [36]. COX-2 is an inducible enzyme, and overexpression of it has been deemed to involve in the pathogenesis of various inflammatory diseases, angiogenesis, and cancer cell

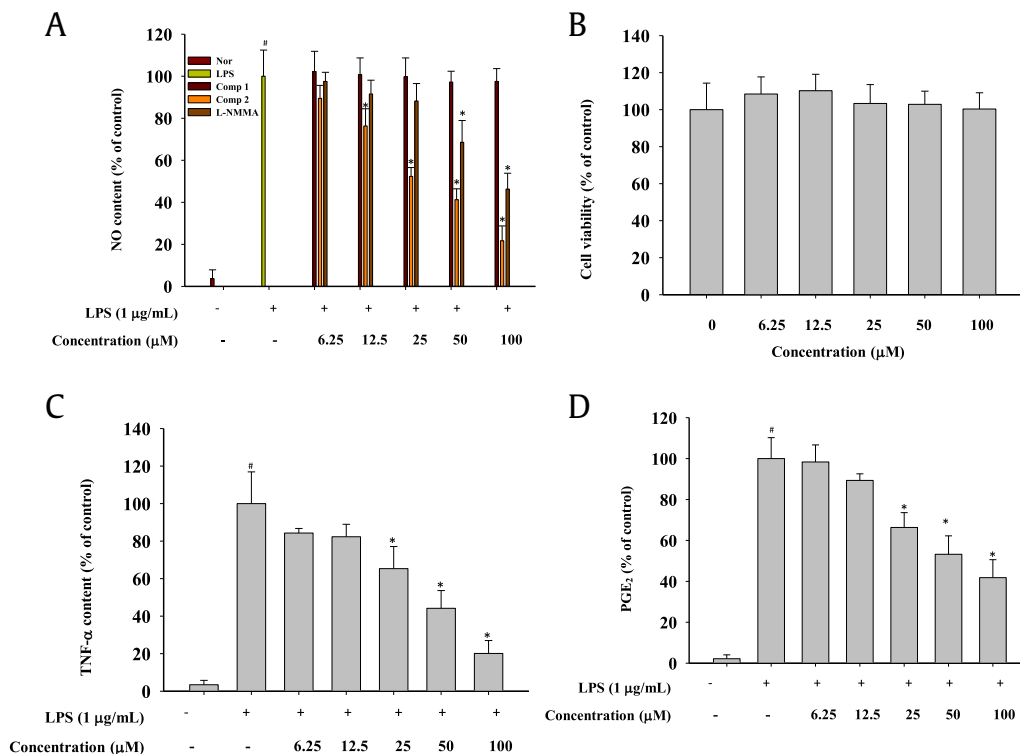


Fig. 3. Inhibitory effect of Compounds 1 and 2 on NO, PGE₂, and TNF- α production. Cells were cultured for 18 h in a 96-well plate; the cells were pretreated with various concentrations of test samples for 30 min before treatment with LPS for 24 h. (A) Nitrite contents were determined by the Griess reaction. (B) Cell viability was investigated by MTT assay. (C and D) TNF- α and PGE₂ were determined using commercial kits according to the manufacturers' instructions. The data are presented as means \pm SD ($n = 3$). * $p < 0.05$ vs LPS⁺ group; # $p < 0.05$ vs control group.

LPS, lipopolysaccharide; MTT, 1-(4,5-dimethylthiazol-2-yl)-3,5-diphenylformazan; NO, nitric oxide; PGE₂, prostaglandin E₂; SD, standard deviation; TNF- α , tumor necrosis factor- α .

invasion [37]. The expression of iNOS and COX-2 induces the generation of excessive amounts of NO and PGE₂ [38]. In the present study, protein expression of iNOS and COX-2 was attenuated by Compound 2 treatment, which might indicate that Compound 2 inhibited the production of NO and PGE₂ by the downregulating protein expression level of iNOS and COX-2 (Fig. 4).

In conclusion, we reported the isolation of two new and minor ginsenosides from the leaves of *P. ginseng* and found that Compound 2 showed excellent antiinflammatory activity. This study might provide further insights into the chemical compositions and functions of the leaves of *P. ginseng* and help to explore this invaluable source.

Conflicts of interest

The authors declare no conflicts of interest.

Acknowledgments

This work was financially supported by the West Light Foundation of Chinese Academy of Sciences (Y7C1031100), Huai'an 2016 Annual Promotion Project for Science and Technology International Cooperation (HAC201620 and HAC201622), National Natural Science Foundation of China (21561142003 and 41501262), Natural Science Foundation of Jiangsu Province (BK20171269 and BK20140455), National Basic Research Program of China (973 Program, 2015CB554400), Natural Science Foundation of the Higher Education Institutions of Jiangsu Province (17KJA550001 and 18KJA550001), and Qing Lan Project of Jiangsu Province.

References

- Oh JY, Kim YJ, Jang MG, Joo SC, Kwon WS, Kim SY, Jung SK, Yang DC. Investigation of ginsenosides in different tissues after elicitor treatment in *Panax ginseng*. *J Ginseng Res* 2014;38:270–7.
- Cheng YJ, Zhang M, Liang QL, Hu P, Wang YM, Jun FW, Luo GA. Two-step preparation of ginsenoside Re, Rb₁, Rc and Rb₂ from the root of *Panax ginseng* by high-performance counter-current chromatography. *Sep Purif Technol* 2011;77:347–54.
- Xie JT, Mehendale SR, Wang A, Aung HH, Wu J, Osinski J, Yuan CS. American ginseng leaf: ginsenoside analysis and hypoglycemic activity. *Pharmacol Res* 2004;49:113–7.
- Li TSC, Mazza G, Cottrell AC, Gao L. Ginsenosides in roots and leaves of American ginseng. *J Agric Food Chem* 1996;44:717–20.
- Leung KW, Pon YL, Wong RNS, Wong AST. Ginsenoside-Rg₁ induces vascular endothelial growth factor expression through the glucocorticoid receptor-related phosphatidylinositol 3-kinase/akt and β -catenin/T-cell factor-dependent pathway in human endothelial cells. *J Biol Chem* 2006;281:36280–8.
- Leung KW, Cheung LWT, Pon YL, Wong RNS, Mak NK, Fan TPD, Au SCI, Tombran-Tink J, Wong AST. Ginsenoside Rb₁ inhibits tube-like structure formation of endothelial cells by regulating pigment epithelium-derived factor through the oestrogen β receptor. *Brit J Pharmacol* 2007;152:207–15.
- Wang HW, Peng DC, Xie JT. Ginseng leaf-stem: bioactive constituents and pharmacological functions. *Chin Med UK* 2009;4:20.
- Liu GY, Li XW, Wang NB, Zhou HY, Wei W, Gui MY, Yang B, Jin YR. Three new dammarane-type triterpene saponins from the leaves of *Panax ginseng* C.A. Meyer. *J Asian Nat Prod Res* 2010;12:865–73.
- Zhu TT, Li F, Chen B, Deng Y, Wang MK, Li LH. Studies on the saponins from the leaves of *Panax ginseng*. *Chin J Appl Environ Biol* 2016;22:70–4.
- Yang XW, Li LY, Tian JM, Zhang ZW, Ye JM, Gu WF. Ginsenoside-Rg₆, a novel triterpenoid saponin from the stem-leaves of *Panax ginseng* C.A. Meyer. *Chin Chem Lett* 2000;11:909–12.
- Cong DL, Song CC, Xu JD. Isolation and identification of 20 (s)-ginsenoside-Rh1, -Rh2 and ginsenoside-Rh3 from the leaves of *Panax quinquefolium*. *Chin Pharm J* 2000;35:82–4.
- Ryu JH, Park JH, Eun JH, Jung JH, Sohn DH. A dammarane glycoside from Korean red ginseng. *Phytochemistry* 1997;44:931–3.
- Park IH, Kim NY, Han SB, Kim JM, Kwon SW, Kim HJ, Park MK, Park JH. Three new dammarane glycosides from heat processed ginseng. *Arch Pharm Res* 2002;25:428–32.
- Ryu JH, Park JH, Kim TH, Sohn DH, Kim JM, Park JH. A genuine dammarane glycoside, (20E)-ginsenoside F₄ from Korean red ginseng. *Arch Pharm Res* 1996;19:335–6.
- Ying A, Yu QT, Guo L, Zhang WS, Liu JF, Li Y, Song H, Li P, Qi LW, Ge YZ, et al. Structural–activity relationship of ginsenosides from steamed ginseng in the treatment of erectile dysfunction. *Am J Chin Med* 2018;1–19.
- Baek SH, Shin BK, Kim NJ, Chang SY, Park JH. Protective effect of ginsenosides Rk₃ and Rh₄ on cisplatin-induced acute kidney injury *in vitro* and *in vivo*. *J Ginseng Res* 2017;41:233–9.
- Wen R, Lv HN, Jiang Y, Tu PF. Anti-inflammatory flavone and chalcone derivatives from the roots of *Pongamia pinnata* (L.) Pierre. *Phytochemistry* 2018;149:56–63.
- Ahmad TB, Liu L, Kokiwi M, Benkendorff K. Review of anti-inflammatory, immune-modulatory and wound healing properties of molluscs. *J Ethnopharmacol* 2018;210:156–78.
- Liu MT, Zhou Q, Wang JP, Liu JJ, Qi CX, Lai YJ, Zhu HC, Xue YB, Hu ZX, Zhang YH. Anti-inflammatory butenolide derivatives from the coral-derived fungus *Aspergillus terreus* and structure revisions of aspernolides D and G, butyrolactone VI and 4',8''-diacetoxy butyrolactone VI. *RSC Adv* 2018;8:13040–7.
- Gao Y, Chu SF, Li JW, Li JP, Zhang Z, Xia CY, Heng Y, Zhang MJ, Hu JF, Wei GN, et al. Anti-inflammatory function of ginsenoside Rg1 on alcoholic hepatitis through glucocorticoid receptor related nuclear factor-kappa B pathway. *J Ethnopharmacol* 2015;173:231–40.
- Kang S, Park SJ, Lee AY, Huang J, Chung HY, Im DS. Ginsenoside Rg3 promotes inflammation resolution through M2 macrophage polarization. *J Ginseng Res* 2018;42:68–74.
- Tam DNH, Truong DH, Nguyen TTH, Quynh LN, Tran L, Nguyen HD, Shamandy B, Le TMH, Tran DK, Sayed D, et al. Ginsenoside Rh1: a systematic review of its pharmacological properties. *Planta Med* 2018;84:139–52.
- Li F, Yang FM, Liu X, Wang L, Chen B, Li LH, Wang MK. Cucurbitane glycosides from the fruit of *Siraitia grosvenori* and their effects on glucose uptake in human HepG2 cells *in vitro*. *Food Chem* 2017;228:567–73.
- Baek KS, Hong YD, Kim Y, Sung NY, Yang S, Lee KM, Park JY, Park JS, Rho HS, Shin SS, et al. Anti-inflammatory activity of AP-SF, a ginsenoside-enriched fraction, from Korean ginseng. *J Ginseng Res* 2015;39:155–61.
- Wang JH, Li X, Wang YJ. A new triterpenoid in the leaves and stems of *Panax quinquefolium* L. from Canada. *J Shenyang Pharm Univ* 1997;14:135–6.
- Wan JB, Zhang QW, Hong SJ, Guan J, Ye WC, Li SP, Simon Lee MY, Wang YT. 5,6-didehydroginsenosides from the roots of *Panax notoginseng*. *Molecules* 2010;15:8169–76.
- Yang H, Kim JY, Kim SO, Yoo YH, Sung SH. Complete ¹H-NMR and ¹³C-NMR spectral analysis of the pairs of 20(S) and 20(R) ginsenosides. *J Ginseng Res* 2014;38:194–202.
- Kmieć Z, Cyman M, Ślebioda TJ. Cells of the innate and adaptive immunity and their interactions in inflammatory bowel disease. *Adv Med Sci* 2017;62(1):1–16.
- Danie IO, Rosina LF. Immunomodulating peptides for food allergy prevention and treatment. *Crit Rev Food Sci Nutr* 2018;58:1629–49.
- Zhu G, Wang H, Wang T, Shi F. Ginsenoside Rg1 attenuates the inflammatory response in DSS-induced mice colitis. *Int Immunopharmacol* 2017;50:1–5.
- Zhang YX, Wang L, Xiao EL, Li SJ, Chen JJ, Gao B, Min GN, Wang ZP, Wu YJ. Ginsenoside-Rd exhibits anti-inflammatory activities through elevation of antioxidant enzyme activities and inhibition of JNK and ERK activation *in vivo*. *Int Immunopharmacol* 2013;17:1094–100.
- Choi WY, Lim HW, Lim CJ. Anti-inflammatory, antioxidative and matrix metalloproteinase inhibitory properties of 20(R)-ginsenoside Rh2 in cultured macrophages and keratinocytes. *J Pharm Pharmacol* 2012;65:310–6.
- Li J, Du J, Liu D, Cheng BB, Fang FF, Weng L, Wang C, Ling CQ. Ginsenoside Rh1 potentiates dexamethasone's anti-inflammatory effects for chronic inflammatory disease by reversing dexamethasone-induced resistance. *Arthritis Res Ther* 2014;16:R106.
- Yu T, Yang YY, Kwak YS, Song GG, Kim MY, Rhee MH, Cho JY. Ginsenoside Rc from *Panax ginseng* exerts anti-inflammatory activity by targeting TANK-binding kinase 1/interferon regulatory factor-3 and p38/ATF-2. *J Ginseng Res* 2017;41:127–33.
- Lee YY, Park JS, Jung JS, Kim DH, Kim HS. Anti-inflammatory effect of ginsenoside Rg5 in lipopolysaccharide-stimulated BV2 microglial cells. *Int J Mol Sci* 2013;14:9820–33.
- Bueno-Silva B, Kawamoto D, Ando-Sugimimoto ES, Casarin RCV, Alencar SM, Rosalen PL, Mayer MPA. Brazilian red propolis effects on peritoneal macrophage activity: nitric oxide, cell viability, pro-inflammatory cytokines and gene expression. *J Ethnopharmacol* 2017;207:100–7.
- Shehzad A, Parveen S, Qureshi M, Subhan F, Lee YS. Decursin and decursinol angelate: molecular mechanism and therapeutic potential in inflammatory diseases. *Inflamm Res* 2018;67:209–18.
- Kim E, Yi YS, Son YJ, Han SY, Kim DH, Nam G, Hossain MA, Kim JH, Park J, Chol JY. BIOGFIK, a compound K-rich fraction of ginseng, plays an anti-inflammatory role by targeting an activator protein-1 signaling pathway in RAW 264.7 macrophage-like cells. *J Ginseng Res* 2018;42(2):233.